

# Fabrication of tungsten tip probes within 3 s by using flame etching

Cite as: Rev. Sci. Instrum. **90**, 063701 (2019); <https://doi.org/10.1063/1.5085251>

Submitted: 11 December 2018 . Accepted: 21 May 2019 . Published Online: 12 June 2019

Takayuki Yamaguchi, Eiichi Inami , Yuto Goto, Yuta Sakai, Satoru Sasaki, Teruaki Ohno , and Toyo Kazu Yamada 



View Online



Export Citation



CrossMark



# Fabrication of tungsten tip probes within 3 s by using flame etching

Cite as: Rev. Sci. Instrum. 90, 063701 (2019); doi: 10.1063/1.5085251

Submitted: 11 December 2018 • Accepted: 21 May 2019 •

Published Online: 12 June 2019



View Online



Export Citation



CrossMark

Takayuki Yamaguchi,<sup>1</sup> Eiichi Inami,<sup>1,2</sup>  Yuto Goto,<sup>1</sup> Yuta Sakai,<sup>1</sup> Satoru Sasaki,<sup>1</sup> Teruaki Ohno,<sup>3</sup>   
and Toyo Kazu Yamada<sup>1,4,a)</sup> 

## AFFILIATIONS

<sup>1</sup>Department of Materials Science, Chiba University, 1-33 Yayoi-cho, Inage-ku, Chiba 263-8522, Japan

<sup>2</sup>School of Systems Engineering, Kochi University of Technology, 185 Miyanokuchi, Tosayamada, Kami, Kochi 782-8502, Japan

<sup>3</sup>Technex Lab Co. Ltd., 8-4-4, Naruse Machida-shi, Tokyo 194-0044, Japan

<sup>4</sup>Molecular Chirality Research Center, Chiba University, 1-33 Yayoi-cho, Inage-ku, Chiba 263-8522, Japan

<sup>a)</sup>E-mail: [toyoyamada@faculty.chiba-u.jp](mailto:toyoyamada@faculty.chiba-u.jp)

## ABSTRACT

A tungsten (W) tip has been used as a standard tip probe because of its robustness at the highest boiling temperature; the use cases include a field emission (FE) electron source for scanning electron microscopy (SEM) and a scanning probe microscopy tip. The W tip probe has generally been fabricated through a chemical etching process with aqueous solutions. In this study, we propose a new method—flame etching. Without using aqueous solutions, a W tip probe was successfully fabricated within 3 s in air, which is very fast and convenient, and beneficial for mass production (additionally, no expensive setup is necessary). A W tip probe was obtained simply by putting a W wire into an oxygen-liquefied petroleum (O<sub>2</sub>+LP) gas flame (giving the highest temperature of ~2300 K) through a microtorch for a few seconds. The obtained W tip provided atomically resolved scanning tunneling microscopic images. Also, since FE electrons were detected by applying ~10<sup>6</sup> V/m, the tip can be used as an FE-SEM source. Generation and vaporization of WO<sub>3</sub> on the W surface are important processes to form a tip shape.

Published under license by AIP Publishing. <https://doi.org/10.1063/1.5085251>

## INTRODUCTION

Tungsten (W) has been used to fabricate a microscopy tip owing to its robustness and extremely high melting point (3695 K). Indeed, the first atomically resolved images were observed using a W tip apex by means of field ion microscopy (FIM) in the 1960s.<sup>1</sup> The W tip has been used as a field-emission emitter of scanning electron microscopy (FE-SEM)<sup>2</sup> and also as one of the standard probes for scanning tunneling microscopy (STM) or atomic force microscopy (AFM) q-plus sensor, which visualize atomic structures of material surfaces and have aided in the development of surface science research.<sup>3–5</sup> Moreover, such a robust W tip was utilized to fabricate a molecule-functionalized tip by picking up a single molecule on top of the W tip, rendering an extremely high-resolution atomic image inside a single organic molecule.<sup>6–8</sup> Furthermore, immiscibility of W with other magnetic metals has enabled us to fabricate a magnetic-film coated W tip, which is widely used to perform spin-polarized STM.<sup>9–13</sup>

The most common method to fabricate this W tip uses chemical etching with aqueous KOH or NaOH solutions (2–5 N).<sup>14–18</sup> This wet etching process was established, but still requires significant knowledge to exclude thick (20–30 nm) oxide films and unknown impurities on the W apex adsorbed from the aqueous solution. Indeed, such adsorbed chemical impurities result in instability of field emission and scanning imaging.<sup>19</sup> The simplest method is rinsing the apex with acetone or hot water, but researchers have developed extra treatments: self-sputtering,<sup>20,21</sup> field evaporation,<sup>22,23</sup> field-assisted etching,<sup>24,25</sup> ion milling,<sup>26</sup> and controllable crashing,<sup>27</sup> in ultrahigh vacuum (UHV) conditions.

In this study, we propose a new method—flame etching. Without any liquid solutions or chemical materials, a W tip probe was successfully fabricated within 3 s in air, which is very fast and convenient, and beneficial for mass production (additionally, no expensive setup is necessary). By simply putting a W wire into a gas-burner flame (~2300 K) through a microtorch within 3 s, a W tip-shape probe was obtained. Because it is known that the wire apex formed

a sphere shape when we heated the W wire apex in a vacuum,<sup>19</sup> the air condition is an important factor in forming the tip shape. Generation and vaporization of  $\text{WO}_3$  were found to be important processes to produce the tip shape. A bare W tip apex was obtained inside the flame due to the extremely high  $\text{WO}_3$  vapor pressure around the tip apex. The obtained W tip provided atomically resolved STM images. Also, since field emission electrons were detected by applying  $\sim 10^6$  V/m, the tip can be used as an FE-SEM source.

## EXPERIMENTAL

A home-built flame etching setup for metal wires is shown in Fig. 1(a). This setup was used only to investigate the flame etching process step by step. We found that such a setup is not necessary, but a W tip was obtained only by putting the wire into the flame for a short period by hand (see [supplementary material](#), movie). The setup consists of a metal wire holder (so-called pin vise) and a microtorch where the flame came out through an aperture with a diameter of 0.5 mm along the  $y$ -direction. A pin vise holding a metal wire was attached to the  $x$ -direction course motion to control smooth linear motion ( $\pm 10$  mm within  $\sim 0.5$  s). Mixed oxygen ( $\text{O}_2$ ) and liquefied petroleum (LP) gas were used for the burner flame

fuel gas. Figure 1(b) shows the burner flame ( $\text{O}_2 + \text{LP}$ ) in our experiment. Depending on the oxygen concentration, the temperature within the flame changes with the distance from the microtorch top  $L$ . In our setup, the inner flame (oxygen-poor white flame) region is  $L \leq 5$  mm, while the outer flame (oxygen-rich blue flame) region is  $L = 5\text{--}43$  mm.<sup>28</sup> The flame temperature was measured using an Ir-IrRh40 thermocouple (Furuya Metal Co., Ltd.) [see Fig. 1(b)]. The highest temperature of  $\sim 2300$  K was measured at  $L \sim 5$  mm. The flame temperature linearly decreased from 2300 K ( $L \sim 5$  mm) to  $\sim 1500$  K ( $L \sim 40$  mm).

Flame etching was performed using metal wires (diameter  $\varphi = 0.1\text{--}0.3$  mm, purity 99.95%). These metal wires were cut off by a nipper with a length of  $15 \pm 5$  mm and then fixed to the pin vise. Using the linear motion controller, the cut edge of the metal wire was inserted into the flame from the  $x$ -direction (perpendicular to the flame direction) [see Fig. 1(c)]. Safety glasses were required. With the setup shown in Fig. 1(a), the period that the wire apex was exposed in the flame was controlled at  $\sim 0.5$  s, while the period can be decreased down to  $\sim 0.1$  s by shaking one hand [without using the setup in Fig. 1(a)].

Chemical identification of the adsorbed species on the flamed W surfaces was performed using X-ray diffraction (XRD) and SEM energy dispersive X-ray (EDX) spectroscopy. XRD data were

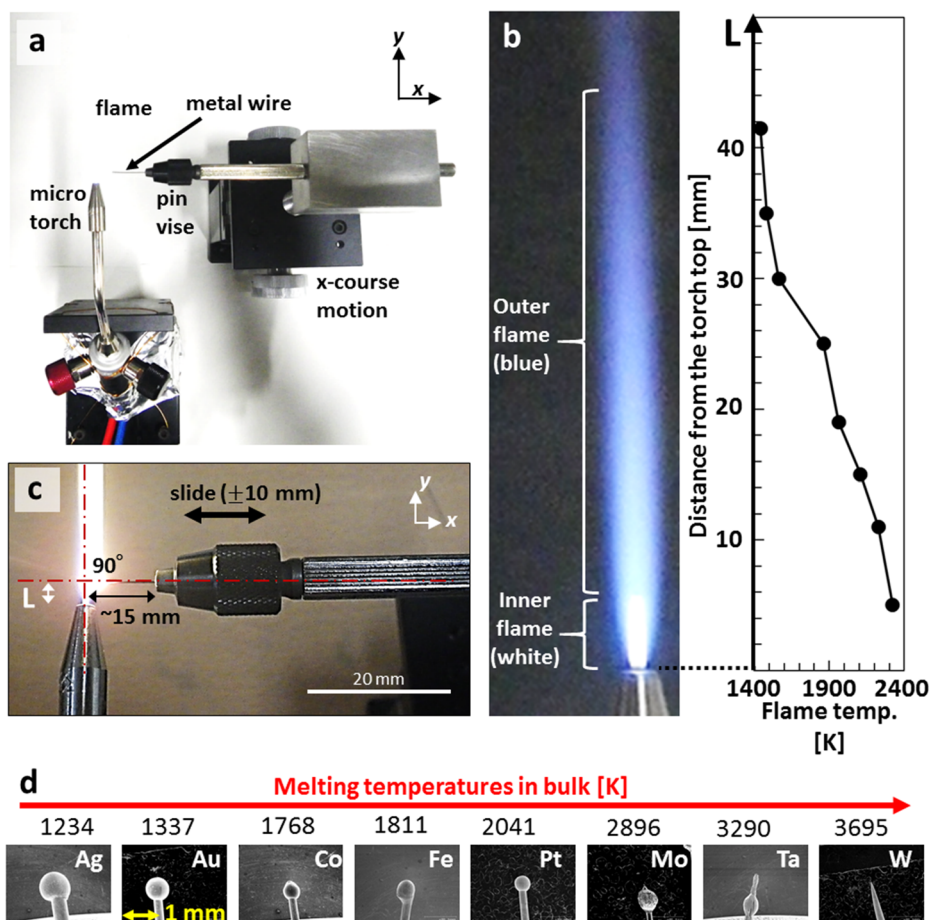


**FIG. 1.** (a) Our flame etching setup consists of flame (LP gas mixed with  $\text{O}_2$  gas) through the microtorch. (b) An enlarged image of the flame. White inner flame ( $L = 0\text{--}5$  mm) and blue outer flame can be observed ( $L = 5\text{--}43$  mm). Temperature inside the flame was measured by using a Ir-IrRh<sub>40</sub> thermocouple. (c) Enlarged image of (a) during the flame etching. (d) SEM images of metal wire edges with different melting temperatures after baking by the flame for 0.5–2.5 s (magnification  $\times 30$ ).

recorded with a Bruker AXS D8 Advance spectrometer (Cu tube, 40 kV). SEM JSM-6510A (JEOL) setup was used to perform EDX measurements. The apex of the wire was characterized by Tiny-SEM (Technex Lab. Co. Ltd.) under pressure of approximately  $10^{-2}$  Pa. The energy of the electron beam was 10 kV.

A home-built ultrahigh vacuum STM setup operated at 300 K was used to test the flame-etched W tip performance. The STM was controlled with Nanonis SPM control system. Obtained STM images were analyzed with WSxM 5.0 Develop 9.0 software (Nanotech Electronica SL). The setup consists of three UHV chambers: introduction (base pressure:  $5 \times 10^{-8}$  Pa), preparation (base pressure:  $1 \times 10^{-8}$  Pa), and analytical chambers (base pressure:  $<1 \times 10^{-8}$  Pa). These chambers were connected by the UHV gate valves. Therefore, the tip was transferred between the chambers without breaking vacuum. The STM was located in the analytical chamber. The flamed-etched W tip prepared in air was introduced from the introduction chamber. The chamber was pumped from atmosphere to  $\sim 10^{-6}$  Pa within 1 h. Then, we opened the gate valve and set the tip into the STM. A Au(110) single crystal surface was used. The fcc-Au(110) surface forms missing row surface reconstruction with a  $p(1 \times 2)$  periodicity. The Au(110) surface was cleaned in the preparation chamber by repeating several cycles of Ar<sup>+</sup> sputtering (0.75 keV) and annealing (743 K). We also tested the tip performance on the Au(110) using the commercial STM setup (JEOL-4200) in air. The flame-etched W tips detected tunneling current without crashing even in air (see [supplementary material](#), Fig. S4). The STM images were obtained by using a constant current mode (feedback on), while the tunneling current as a function of the sample bias voltage [ $I(V)$  curve] was measured by keeping the tip-sample separation (feedback off).

## RESULTS AND DISCUSSION

### Flame etching of various metal wires

First, we placed various metal wire edges into the flame for 0.5–2.5 s at  $L \sim 5$  mm ( $\sim 2300$  K). [Figure 1\(d\)](#) shows the obtained edges after baking. Because Au, Ag, Co, Fe, and Pt have lower melting temperatures in bulk, the edges formed a sphere shape due to local melting. Interestingly, Mo and Ta wires also formed a sphere ball shape while their melting temperature in bulk is higher than the flame temperature of 2300 K. However, markedly, W wire with the highest melting temperature of 3695 K in bulk formed a tip shape. This unexpected result was the starting point of this flame etching study.

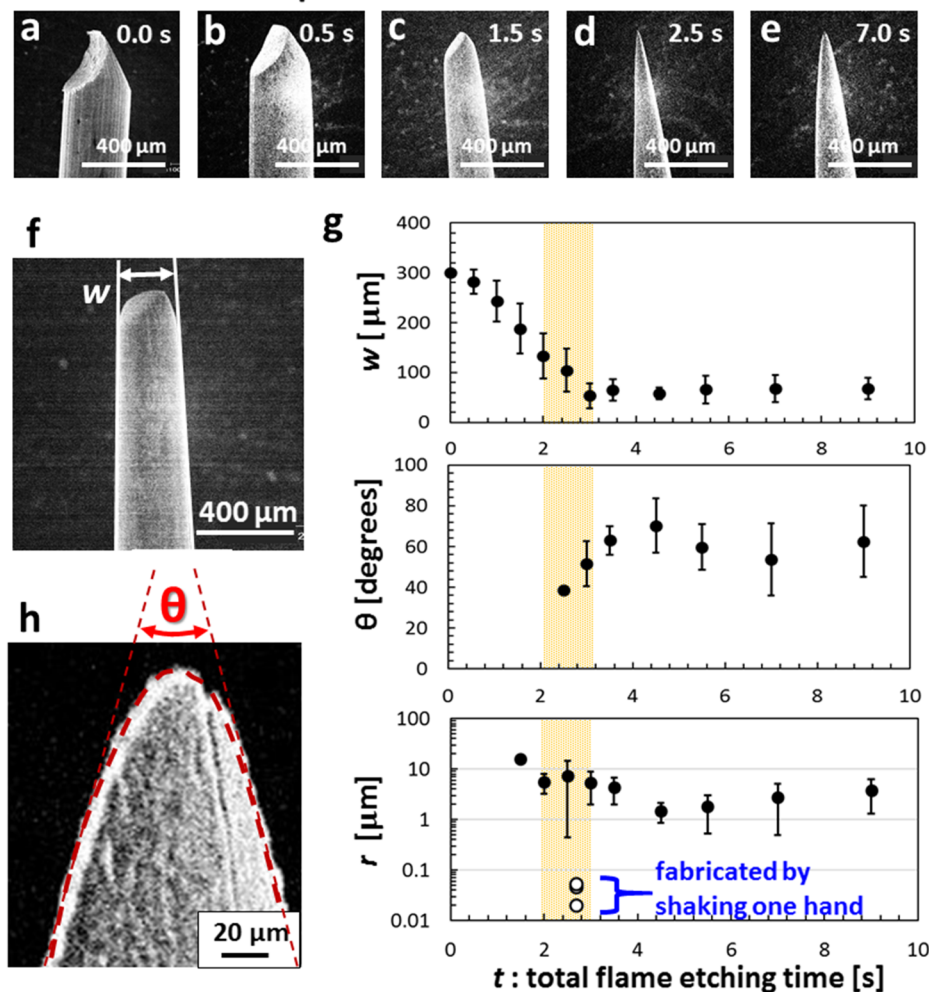
### Flame etching for W wires

[Figure 2](#) shows a systematic study of the flame etching of the W wires using the setup in [Fig. 1](#). We studied how the shape of the W wire apex changes with an increase in the total flame etching time  $t$  ( $O_2+LP$  gas,  $L = 5$  mm). Strong light flashed during the flame etching. Indeed, this flashing is an important signature for successful flame etching. Without strong flashing light, no etching occurred. We started to count time when the wire apex was placed at the center of the flame ( $t = 0$  s) [see [Fig. 1\(c\)](#)]. [Figures 2\(a\)–2\(e\)](#) show SEM images of one W wire. Before the flame etching, the W wire exhibited sharply cut edge [see [Fig. 2\(a\)](#)]. However, only 0.5 s of flame etching rendered the edge rounder [[Fig. 2\(b\)](#)]. We continued the etching

and checked the edge shape every 0.5 s. Drastic change occurred at  $t = 1.5$  s [[Fig. 2\(c\)](#)]. Here, the wire body shrank to  $\sim 50\%$ . Additionally, the apex started narrowing. Markedly, at  $t = 2.5$  s [[Fig. 2\(d\)](#)], the apex changed to a tip shape. Once the tip shape was formed, further baking did not significantly change the shape [see [Fig. 2\(e\)](#),  $t = 7.0$  s]. We repeated the flame etching for 9 W wires and checked the apex shape every 0.5 s with, in total, 99 SEM images (see [supplementary material](#), Fig. S1). Markedly, all W wires formed a tip shape, promising good reproducibility. These consecutive results demonstrate that the present flame etching method is capable of fabricating a W tip within a few seconds.

To obtain deeper insights into the tip formation, we have statistically analyzed the obtained SEM images. In this analysis, we quantitatively characterize the wire shape by three parameters: the body diameter of the wire  $w$ , cone angle of the apex  $\theta$ , and the tip radius  $r$ . The body diameter  $w$  is defined as the distance between solid lines in [Fig. 2\(f\)](#) at the foremost tip apex. The tip radius  $r$  is the radius of local curvature at the foremost tip apex [see [Fig. 2\(h\)](#)], which was obtained by parabolic curve fitting:  $y = ax^2 + bx + c$  and  $r = (2a)^{-1}$ .<sup>29</sup> [Figure 2\(g\)](#) shows the obtained  $w$ ,  $\theta$ , and  $r$  values as a function of  $t$ . More and more flame etching decreased the  $w$  value starting from 300  $\mu\text{m}$  to  $\sim 50$   $\mu\text{m}$  within 3 s. However, additional etching did not change the  $w$  values. Angle  $\theta$  was able to measure from  $t = 2.5$  s when the tip shape was formed. Starting from  $40^\circ$ , it increased to approximately  $60^\circ$  by further flame etching. The tip radius  $r$  values decreased below  $\sim 10$   $\mu\text{m}$  within  $t \sim 2$  s. Using the setup in [Fig. 1](#), the radius was typically 0.5–5  $\mu\text{m}$  by further flame etching.

From this statistical experimental analysis, W wire apices with narrow body ( $w < 100$   $\mu\text{m}$ ), small cone angle ( $\sim 40^\circ$ ), and small tip radius ( $r \sim 1$   $\mu\text{m}$ ) were obtained around  $t \sim 2.5$ –3.0 s with a higher probability. However, using the setup in [Fig. 1](#), it was difficult to obtain the apex with a radius lower than 1  $\mu\text{m}$ . We expected that a sharper tip could be fabricated between  $t \sim 2.5$  and 3.0 s. Then, we further performed the flame etching by shaking one hand as fast as possible. This swift flame etching gave a short flame etching period of  $\sim 0.1$  s. First, we placed the W wire into the flame for  $t \sim 2.5$  s and obtained the tip shape with a narrow body. Next, we inserted the apex, using one hand, into the flame every  $\sim 0.1$  s ( $L \sim 5 \pm 1$  mm) for 1–3 times. The W tip apices before and after the  $\sim 0.1$  s flame etching are shown in [Fig. 3\(a\)](#). The blunter apex was drastically sharpened and several grains can be observed, i.e., the apex has a polygonal shape. Because a similar shape was observed at the tip apex fabricated from the single crystalline W wire,<sup>19</sup> the flame etched W apex could include several single crystal grains. To measure the local curvature of such an apex, we performed field emission curve measurements in a vacuum using the setup in Ref. 19. [Figure 3\(b\)](#) shows the obtained results. Because the W tip surface was coated by thin oxide layers, a gentle annealing of 1500–2300 K (30–40 W) was performed. The W tip radius is known to not be melted by this annealing.<sup>19</sup> We observed the onset of the field emission currents around 1000–2000 eV. From the Fowler-Nordheim (F-N) fitting, we found the tip radius of  $r \sim 20$ –52 nm at  $t \sim 2.7$  s [open circles in [Fig. 2\(g\)](#)]. The differences between the F-N fitting curves and the experimentally obtained data could be because of using the semispherical apex model for the F-N plot, while the obtained W tip apex had polygonal grains [see [Fig. 3\(a\)](#)]. Since field emission electrons were obtained with an application of the

Flame-etched W tips at  $L = 5$  mm

**FIG. 2.** (a)–(e) SEM images of the W wire after the flame etching. Total flame etching time is (a) 0 s, (b) 0.5 s, (c) 1.5 s, (d) 2.5 s, and (e) 7.0 s. (f) The body diameter of W wire ( $w$ ) was obtained by setting two straight lines along the body of the wire and measured the distance between the lines at the apex position. (g) Dependence of the body diameter ( $w$ ), the cone angle ( $\theta$ ), and the tip radius ( $r$ ) of the W wires on the total flame etching time ( $t$ ). Sharper tips were fabricated with swift flame etching by shaking one hand (white circles). Radii of the obtained W tips were evaluated from the field emission curves in Fig. 3. (h) The tip radii in (g) (black dots) were simply obtained by fitting the parabolic function to the tip apex in the SEM image:  $ax^2 + bx + c$ ,  $r \sim (2a)^{-1}$ .

electric field:  $\sim 10^6$  V/m ( $= 1$  kV/1 mm), the obtained W tip can be used as a field emission scanning electron microscopy (FE-SEM) source.

Further, the obtained sharper W tip was tested as an STM probe [see Figs. 3(c)–3(e)]. The flame-etched W tip was immediately set to the UHV-STM setup at 300 K. Figure 3(c) shows an STM topographic image obtained on the Au(110) surface in UHV at 300 K. Several atomic terraces are observed. The line profile along the arrow (left to right) in Fig. 3(c) showed  $\sim 150$  pm height steps [see the lower panel in Fig. 3(c)], which is in agreement with the bulk fcc Au(110) plane distance of 144 pm. One dimensional lines along  $\langle 110 \rangle$  direction show the fcc-Au(110)  $p(1 \times 2)$  missing row pattern. The enlarged image [Fig. 3(d)] shows the atomic structure on the reconstructed surface. The line profile along the arrow (top to bottom) in Fig. 3(d) shows periodic peaks with an interval of  $\sim 0.8$  nm, corresponding to the  $p(1 \times 2)$  structure of  $408 \times 2 = 816$  pm.

Tunneling current as a function of sample bias voltage [ $I(V)$  curve] was measured on the Au surface [see Fig. 3(e)]. The obtained

$I(V)$  curve shows an exponential increase from 0 V (= the Fermi energy) to both positive and negative bias voltages. Positive and negative voltage sides denote sample and tip density of states, respectively, i.e., the tip has no gap around the Fermi energy, ensuring that the flame-etched W tip apex has metallic property.

The flames etched W tips were also examined by using the air STM (JEOL-4200). The tip detected tunneling current without a crash even in air (see supplementary material, Fig. S4). This proves that the oxidization on the apex was not significant.

### Flame etching mechanism through $\text{WO}_3$ generation and vaporization

Although we demonstrated the usefulness and convenience of the flame etching to change the W wire to the tip shape, there is still curiosity in the mechanism itself. One might think that the etching occurs by vaporization of the W atoms from the surface. However, this cannot be the major driving force. This is because W has an

## Flame-etched W tips by shaking one hand

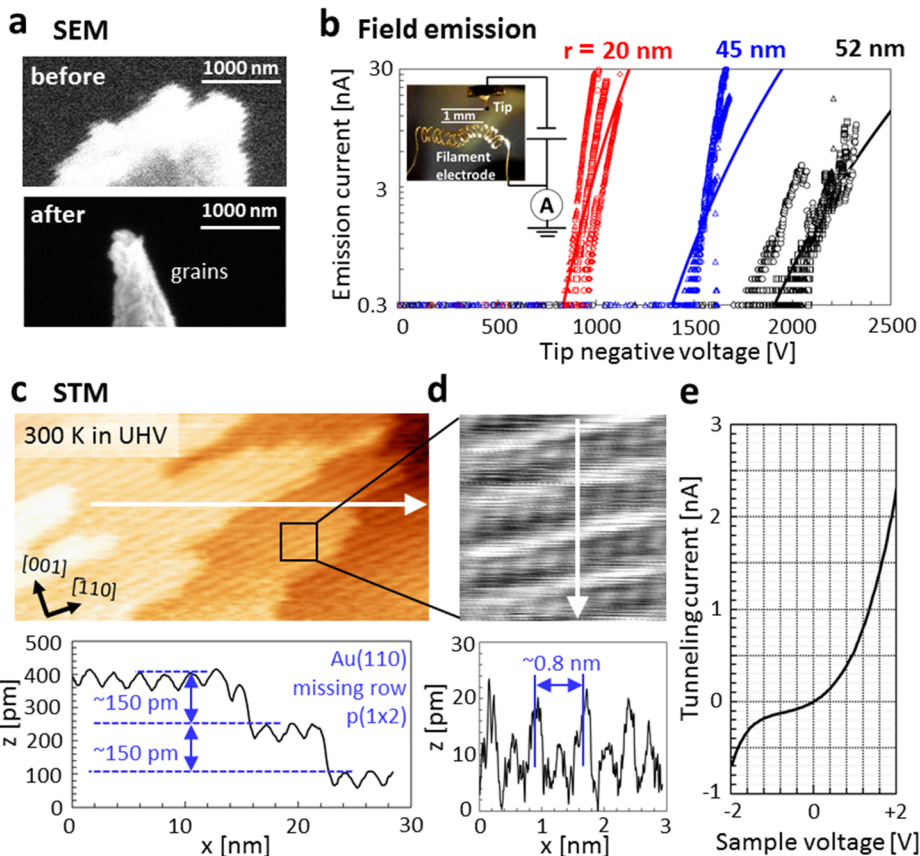


**FIG. 3.** (a) SEM images of a W tip apex fabricated before (upper panel) and after (lower panel) the swift flame etching ( $\sim 0.1$  s) at  $L = 5$  mm by shaking one hand. The tip etched already with LP+O<sub>2</sub> gas flame at  $L \sim 5$  mm for  $\sim 2$  s ( $\sim 2300$  K) was used. (b) Field emission curves obtained from the flame-etched tips by shaking one hand. We tested three different tips (red, blue, and black). The fitted Fowler-Nordheim plots (solid lines) show the tip radii of 20, 45, and 52 nm, respectively. The inset shows the W tip and the counter filament electrode inside UHV setup. (c) An STM topographic image (raw data, no filtering, only local plane background subtraction) obtained on a fcc-Au(110) surface at 300 K in UHV by using the flame-etched W tip ( $35 \times 17 \text{ nm}^2$ ,  $V_s = -90 \text{ mV}$ ,  $I_t = 1 \text{ nA}$ ). The lower panel denotes the line profile along the white arrow. (d) The enlarged STM image of the boxed area in (c) ( $3 \times 3 \text{ nm}^2$ ,  $V_s = -9 \text{ mV}$ ,  $I_t = 1 \text{ nA}$ ; raw data, no filtering, only local plane background subtraction). The lower panel denotes the line profile along the arrow. (e) Tunneling current as a function of the sample bias voltage [ $I(V)$  curve] obtained on the Au surface showing no gap around the Fermi energy.

extremely high melting temperature (3695 K) [see Fig. 1(d)] and very low vapor pressure:  $10^{-8}$  Torr even at  $\sim 2400$  K,<sup>30</sup> which is comparable to that of the LP gas flame at  $L \sim 5$  mm [see Fig. 1(b)]. Additionally, in UHV, the 1500–2300 K annealing (30–40 W) removes the oxide films covered on the W tips apex, while the powerful  $>2300$  K annealing (50–60 W) makes the apex radius larger (see Ref. 19), i.e., the annealing in UHV enhances the diffusion of the W atoms at the apex and makes the tip apex blunter. However, in air, the flame etching indeed changed the wire edge to the tip shape, indicating precursor reactions between W atoms and air could be necessary for the flame etching.

The mechanism of the flame etching of the W wire was understood while testing the etching process at different flame positions. The results in Figs. 1–3 were obtained at  $L = 5$  mm, but here we put the wire at  $L = 35$  mm (the oxygen-rich outer flame with lower temperature: around the center  $\sim 1500$  K, while the outside  $\sim 1200$  K [see Fig. 1(b) and Ref. 28]). Still we observed strong flashing, and the W wire apex formed a tip shape (see supplementary material, Fig. S2a). However, we found visually that the W wire surface was coated by yellowish powders. Because the powders were easily peeled off, we collected them and the powder XRD data were obtained, as shown in Fig. 4(a) ( $L = 35$  mm). There is in agreement between the yellowish powders and monoclinic WO<sub>3</sub> XRD reference data

(No. 80056-ICSD), e.g., the XRD intensity peaks at  $2\theta = 23.7^\circ$ ,  $34.3^\circ$ , and  $50.1^\circ$  correspond to (020), (201), and (140) crystalline planes, respectively.<sup>31</sup> Therefore, the obtained yellowish powder on the W surface can be identified as WO<sub>3</sub>. This is supported by the fact that the WO<sub>3</sub> is generated at  $\sim 1200$  K in oxygen atmosphere on the W surface.<sup>32</sup> Enlarged SEM images of a W tip etched at  $L = 35$  mm are shown in Fig. 4(b). For every  $\sim 0.5$  mm from the tip apex, we separated four regions, namely I, II, III, and IV. Regions II and III have  $\sim 1 \mu\text{m}$  size domains in agreement with the reported size of  $\sim 0.8 \mu\text{m}$ ,<sup>32</sup> and domain size becomes large and scratches are also observed in region IV. These features indicate that the WO<sub>3</sub> film is thicker apart from the apex. Even visually, we observed that region I has metallic color, while regions II, III, and IV have a yellowish color.

More detailed information on the amount of the WO<sub>3</sub> powder was obtained by SEM-EDX measurements. Figure 4(c) shows energy dispersive X-ray (EDX) spectra obtained at regions I, II, III, and IV (flame etching at  $L = 35$  mm). A clear oxygen peak was observed with two W peaks. However, the oxygen peak becomes small at region I. EDX quantitative analysis results are summarized in the table in Fig. 4(d), where oxygen is one the majority elements (W: 18%–27% and O: 56%–73%) at regions II, III, and IV, while W becomes the majority element (W: 70% and O: 30%) and the amount

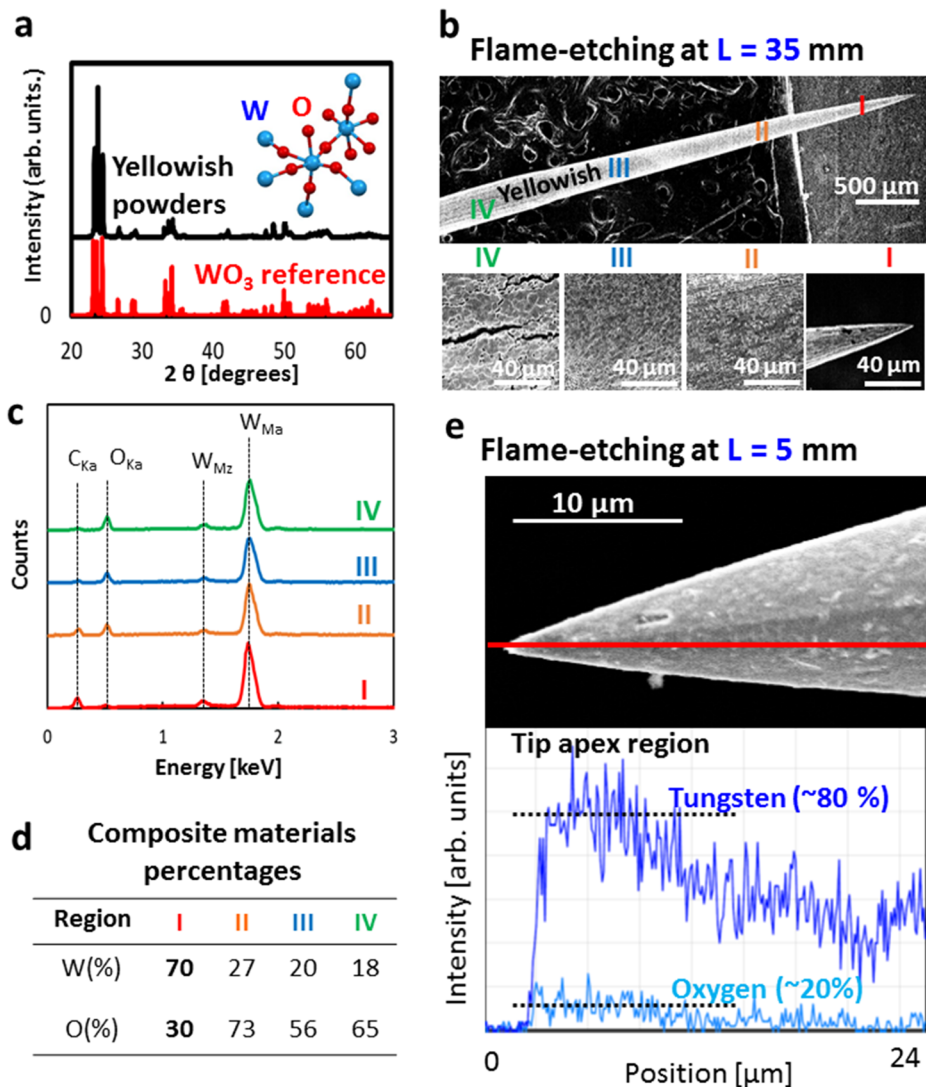


**FIG. 4.** (a)–(d) Tungsten trioxide ( $\text{WO}_3$ ) generation by lower temperature flame (1200–1500 K) at  $L = 35$  mm. (a) X-ray diffraction results of the obtained yellowish powders on the W wires (black line) and monoclinic  $\text{WO}_3$  as a reference (red line). The inset denotes  $\text{WO}_3$  structure model. (b) A SEM image of the flame-etched W tip at  $L = 35$  mm. Enlarged SEM images at regions I, II, III, and IV. (c) SEM-EDX spectra obtained at the regions I, II, III, and IV. (d) Percentages of the composite materials at regions I, II, III, and IV. (e) Upper panel: SEM image obtained at the apex of the W tip flame-etched at  $L = 5$  mm. Lower panel: SEM-EDX measurements obtained along the line in the SEM image.

of oxygen drastically decreases in region I (in the EDX spectrum obtained at region I, one might note that the carbon peak increased, but this could be due to the background sample plate behind the W tip). These experimental results strongly suggest that (1)  $\text{WO}_3$  is indeed generated around 1200 K<sup>32</sup> during the flame etching, and however, (2) around the center of the flame at  $L = 35$  mm ( $\sim 1500$  K) where the tip apex (region I) is located, the  $\text{WO}_3$  vaporization rate is higher than the  $\text{WO}_3$  generation rate, reducing the oxide film thickness.

The yellowish  $\text{WO}_3$  generation was also confirmed using further lower temperature flames. When we put the W wire into the LP+ $\text{O}_2$  gas at  $L \sim 50$  mm, no flashing occurred and no tip shape was obtained (see [supplementary material](#), Fig. S2b). However, the whole W surface exposed in the flame was coated by the same yellowish color, i.e., the W surface could be approximately  $\sim 1200$  K, at which temperature the  $\text{WO}_3$  vaporization rate is smaller than the  $\text{WO}_3$  generation rate.

Here, we emphasize that such yellowish  $\text{WO}_3$  films were not observed for the flame etching at  $L = 5$  mm with the  $\text{O}_2$ +LP flame shown in [Figs. 1–3](#) ( $\sim 2300$  K). The important point is that the  $\text{WO}_3$  has extremely high vapor pressures at  $\sim 1900$  K: 0.001 Torr at  $\sim 1300$  K, 10 Torr at  $\sim 1700$  K, 100 Torr at  $\sim 1800$  K, and 760 Torr at  $\sim 1900$  K,<sup>30</sup> i.e., with the LP+ $\text{O}_2$  flame, the  $\text{WO}_3$  vaporization rate is enhanced and therefore at  $L = 5$  mm, the generated  $\text{WO}_3$  is almost completely vaporized, producing a bare W surface inside the flame ( $\text{WO}_3$  melting point: 1746 K<sup>30</sup>). The demonstrations of the lower-temperature flame etching at  $L = 35$  mm confirmed that  $\text{WO}_3$  generation and vaporization could be the key to producing the tip shape and suggested small amounts of  $\text{WO}_3$  around the apex owing to the higher vaporization rate by higher temperatures at the center of the flame. Namely, the thickness of the oxide films around the apex could be negligibly small for the flame-etched W tip obtained at  $L = 5$  mm. Thus, SEM-EDX measurements were performed at the apex region ( $\sim 10$   $\mu\text{m}$ ), fabricated using the highest flame

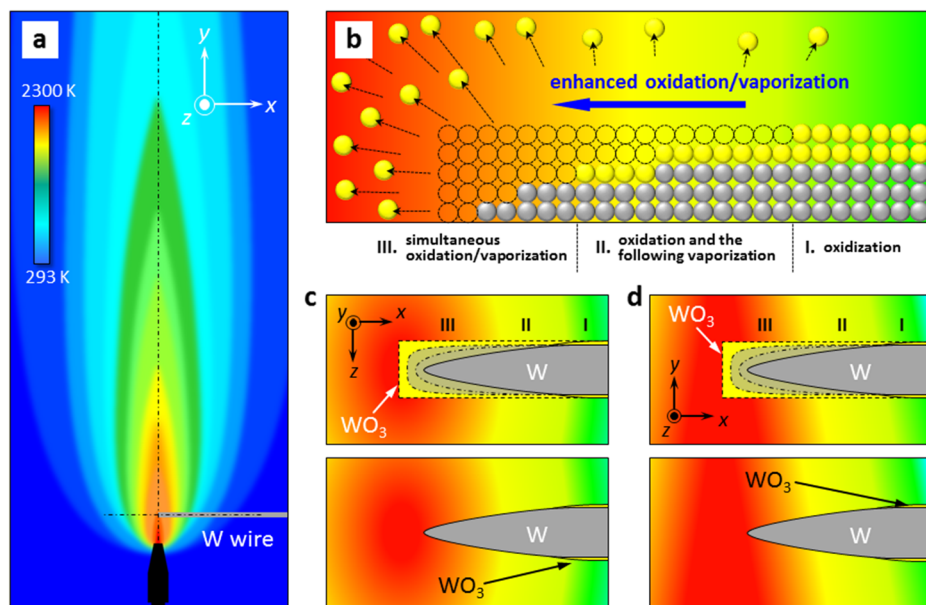


**FIG. 5.** Schematic illustrations, representing W tip formation by flame etching of a W wire with LP+O<sub>2</sub> gas flame. (a) Flame etching setup of a W wire with LP+O<sub>2</sub> gas flame. The color shows temperature distribution of the flame. (b) Close-up view of the W wire edge in (a), representing temperature-dependent WO<sub>3</sub> generation and vaporization. Gray balls represent W, while yellow balls represent WO<sub>3</sub>. [(c) and (d)] Tip formation at the W-wire edge viewed from (c) y- and (d) z-directions in (a). Top (bottom) panels in (c) and (d) show shape of the W wire before (after) the etching inside the flame.

temperature [ $L = 5$  mm, see Fig. 4(e)]. The lower panel in Fig. 4(e) shows EDX signals along the red line in the SEM image in Fig. 4(e). The apex of the flame-etched W tips at  $L = 5$  mm consists of 80% W and 20% O. The O percentage decreased from  $\sim 30\%$  [Fig. 4(d)] to  $\sim 20\%$  [Fig. 4(e)]. Although precise amounts of the remained WO<sub>3</sub> around the apex cannot be determined by the SEM-EDX, the remained WO<sub>3</sub> around the apex is not serious for use in STM/STS probes and FE sources (as demonstrated in Fig. 3).

Based on these results, the mechanism of flame etching was modeled as in Fig. 5, which simply sketches how the flame etching produces a tip shape through WO<sub>3</sub> generation and the subsequent vaporization. By inserting the W wire into the center of the LP+O<sub>2</sub> gas flame at  $L = 5$  mm, the temperature around the wire edge increases depending on the position due to the temperature gradient in the flame [Fig. 5(a)]. This leads to different rates of WO<sub>3</sub> generation and the following vaporization, as shown in Fig. 5(b), which we suggest is crucial to produce a tip shape, as follows. Around the body of the wire [region I in Fig. 5(b)], the W surface oxidizes to be WO<sub>3</sub>, while the vaporization rate is negligibly small due to the low temperature (approximately 1200 K). Therefore, the dominant process is WO<sub>3</sub> generation, and the wire surface is only covered by the WO<sub>3</sub> powder without being etched (reducing the volume of the wire), as shown in Figs. 5(c) and 5(d). Conversely, around the wire surface nearer to the flame center [region II in Fig. 5(b)], WO<sub>3</sub> is not only generated but also starts to be vaporized with higher temperature. This means that the surface starts to be etched. By increasing the temperature of the W surface from region II to region III in Fig. 5(b), the corresponding vaporization rate also increases. Because the vaporization rate, which is given by Arrhenius reaction law, should increase exponentially with temperature, the vaporization at the wire edge (region III) where the temperature is increased up to 2300 K should be dramatically enhanced, and the rate should be limited by the WO<sub>3</sub> generation process. Therefore, at region III, the WO<sub>3</sub> generated should be immediately vaporized, and thus the

etching rate is also enhanced to successfully produce the tip shape [Figs. 5(c) and 5(d)]. We also suggest that such simultaneous W oxidation and vaporization at the flame center are essential to eliminate WO<sub>3</sub> from the wire surface, by which the almost bare W tip apex can be obtained.

One should note that this flame etching method is performed in air. Therefore, even once the bare W surface is exposed inside the flame, the surface is slightly oxidized. Because the WO<sub>3</sub> is produced around 1200 K, it is better to pull out the tip from the flame as fast as possible. This is one reason that the flame etching by shaking one hand produced a sharper tip with a thinner oxide film coating.

## CONCLUSIONS

A W tip was found to be fabricated in air within a few seconds just by placing the W wire into the O<sub>2</sub>+LP gas flame ( $\sim 2300$  K) through the microtorch, which is very fast and convenient, and beneficial for mass production (100 W tips within 30 min, and no expensive setup is necessary). First, the W wire was placed inside the flame for  $t \sim 2.5$  s (strong flashing occurred). Then, the wire apex diameter was reduced from 0.3 mm to 0.1 mm. Subsequently, shaking the wire by one hand, we placed the wire apex only  $\sim 0.1$  s inside the flame. We repeated this several times (total flame etching time:  $t \sim 2.7$  s) and obtained a tip-shape apex. The obtained W tip provided atomically resolved STM images. Also, since field emission electrons were detected by applying the electric field of  $\sim 10^6$  V/m, the tip can be used as a FE-SEM source. Tunneling spectroscopy curves showed no gap at the Fermi energy (i.e., metallic property), and X-ray and SEM-EDX measurements revealed that WO<sub>3</sub> generation and simultaneous vaporization at the W surface inside the flame are the driving force to fabricate the apex with a tip shape. Thus, the flame-etched W tips could be very useful for STM or AFM q-plus sensor probes working in air or liquid conditions.

## SUPPLEMENTARY MATERIAL

See [supplementary material](#) for Fig. S1—Flame etching processes of nine W wires (No. 1–9) obtained at the total flame etching time of 0.5 s, 1.0 s, 1.5 s, 2.0 s, 2.5 s, 3.0 s, 3.5 s, 4.5 s, 5.5 s, 7.0 s, and 9.0 s. Total 99 SEM images; Fig. S2—Flame etching for the W wire at  $L = 35$  mm and 50 mm; Fig. S3—Flame etching for PtIr, Ni, and Ta wires; Fig. S4—STM measurements in air using the flame-etched W tip; and Supplementary video during the W tip flame etching: [http://adv.chiba-u.jp/nano/yamada-upload/20171130\\_flameetching.mp4](http://adv.chiba-u.jp/nano/yamada-upload/20171130_flameetching.mp4).

## ACKNOWLEDGMENTS

This work was supported by JSPS KAKENHI (Grant Nos. 25110011, 15K13357, 16K17521, 16K05887, 17H05353, and 17K19023). E.I. and T.K.Y. acknowledge financial support from the Murata Science Foundation and Hitachi Metals—Materials Science Foundation. We thank Mr. Ryohei Nemoto, Mr. Kenta Yokota, and Mr. Masataka Yamaguchi for technical support of field emission curves and STM measurements. We acknowledge Mr. Ryohei Nemoto, Mr. Nana K. M. Nazriq, and Ms. Kumi Kobayashi for careful reading of our manuscript.

## REFERENCES

- 1 E. W. Mueller, "Das feldionenmikroskop," *Z. Phys.* **131**, 136 (1951).
- 2 J. Pawley, "The development of field-emission scanning electron microscopy for imaging biological surfaces," *Scanning* **19**, 324–336 (1997).
- 3 L. Gerhard, T. K. Yamada, T. Balashov, A. F. Takacs, M. Daena, S. Ostanin, A. Ernst, I. Mertig, and W. Wulfhekel, "Magneto-electric coupling at metal surfaces," *Nat. Nanotechnol.* **5**, 792 (2010).
- 4 E. Inami, M. Shimasaki, H. Yorimitsu, and T. K. Yamada, "Room temperature stable film formation of  $\pi$ -conjugated organic molecules on 3d magnetic substrate," *Sci. Rep.* **8**, 353 (2018).
- 5 T. K. Yamada, Y. Yamagishi, S. Nakashima, Y. Kitaoka, and K. Nakamura, "Role of  $\pi$ -d hybridization in 300-K organic-magnetic interface: Metal-free phthalocyanine single molecules on bcc Fe(001)-whisker," *Phys. Rev. B* **94**, 195437 (2016).
- 6 J. Welker and F. J. Giessibl, "Revealing the angular symmetry of chemical bonds by atomic force microscopy," *Science* **336**, 444–449 (2012).
- 7 L. Gross, F. Mohn, N. Moll, P. Liljeroth, and G. Meyer, "The chemical structure of a molecule resolved by atomic force microscopy," *Science* **325**, 1110–1114 (2009).
- 8 K. M. Nazriq, Nana, E. Minamitani, and T. K. Yamada, "CO-tip manipulation using repulsive interactions," *Nanotechnology* **29**, 495701 (2018).
- 9 T. Irisawa, T. K. Yamada, and T. Mizoguchi, "Spin polarization vectors of field emitted electrons from apexes of Fe-coated W tips," *New J. Phys.* **11**, 113031 (2009).
- 10 T. K. Yamada and A. L. Vazquez de Parga, "Room temperature spin-polarizations of Mn-based antiferromagnetic nanoelectrodes," *Appl. Phys. Lett.* **105**, 183109 (2014).
- 11 T. K. Yamada, M. M. J. Bischoff, G. M. M. Heijnen, T. Mizoguchi, and H. van Kempen, "Observation of spin-polarized surface states on ultrathin bct Mn(001) films by spin-polarized scanning tunneling spectroscopy," *Phys. Rev. Lett.* **90**, 056803-1 (2003).
- 12 T. K. Yamada, M. M. J. Bischoff, T. Mizoguchi, and H. van Kempen, "Use of voltage pulses to detect spin-polarized tunneling," *Appl. Phys. Lett.* **82**, 1437–1439 (2003).
- 13 T. K. Yamada, E. Martinez, A. Vega, R. Robles, D. Stoeffler, A. L. Vazquez de Parga, T. Mizoguchi, and H. van Kempen, "Spin configuration in a frustrated ferromagnetic/antiferromagnetic thin-film system," *Nanotechnology* **18**, 235702 (2007).
- 14 A. I. Oliva, A. Romero G., J. L. Pena, E. Anguiano, and M. Aguilar, "Electrochemical preparation of tungsten tips for a scanning tunneling microscope," *Rev. Sci. Instrum.* **67**, 1917 (1996).
- 15 O. L. Guise, J. W. Ahner, M.-C. Jung, P. C. Goughnour, and J. T. Yates, Jr., "Reproducible electrochemical etching of tungsten probe tips," *Nano Lett.* **2**, 191 (2002).
- 16 M. Kulakov, I. Luzinov, and K. G. Kornev, "Capillary and surface effects in the formation of nanosharp tungsten tips by electropolishing," *Langmuir* **25**, 4462 (2009).
- 17 W. T. Chang, I. S. Hwang, M. T. Chang, C. Y. Lin, W. H. Hsu, and J. L. Hou, "Method of electrochemical etching of tungsten tips with controllable profiles," *Rev. Sci. Instrum.* **83**, 083704 (2012).
- 18 Y. Khan, H. Al-Falih, Y. Zhang, T. K. Ng, and B. S. Ooi, "Two-step controllable electrochemical etching of tungsten scanning probe microscopy tips," *Rev. Sci. Instrum.* **83**, 063708 (2012).
- 19 T. K. Yamada *et al.*, "Electron-bombarded (110)-oriented tungsten tips for stable tunneling electron emission," *Rev. Sci. Instrum.* **87**, 033703 (2016).
- 20 I. Ekvall, E. Wahlstrom, D. Claesson, H. Olin, and E. Olsson, "Preparation and characterization of electrochemically etched W tips for STM," *Meas. Sci. Technol.* **10**, 11 (1999).
- 21 G. J. de Raad, P. M. Koenraad, and J. H. Wolter, "Use of the Schiller decapitation process for the manufacture of high quality tungsten scanning tunneling microscopy tips," *J. Vac. Sci. Technol., B* **17**, 1946 (1999).
- 22 A.-S. Lucier, H. Mortensen, Y. Sun, and P. Grütter, "Determination of the atomic structure of scanning probe microscopy tungsten tips by field ion microscopy," *Phys. Rev. B* **72**, 235420 (2005).
- 23 J. Onoda and S. Mizuno, "Fabrication of (110) oriented tungsten nano-tips by field-assisted water etching," *Appl. Surf. Sci.* **257**, 8427 (2011).
- 24 J. Onoda, S. Mizuno, and H. Ago, "STEM observation of tungsten tips sharpened by field-assisted oxygen etching," *Surf. Sci.* **604**, 1094 (2010).
- 25 C. Vesa, R. Urban, J. L. Pitters, and R. A. Wolkow, "Robustness of tungsten single atom tips to thermal treatment and air exposure," *Appl. Surf. Sci.* **300**, 16 (2014).
- 26 A. N. Chaika, N. N. Orlova, V. N. Semenov, E. Yu. Postnova, S. A. Krasnikov, M. G. Lazarev, S. V. Chekmazov, V. Yu. Aristov, V. G. Glebovsky, S. I. Bozhko, and I. V. Shvets, "Fabrication of [001]-oriented tungsten tips for high resolution scanning tunneling microscopy," *Sci. Rep.* **4**, 3742 (2014).
- 27 M. M. J. Bischoff, T. K. Yamada, C. M. Fang, R. A. de Groot, and H. van Kempen, "Local electronic structure of Fe(001) surfaces studied by scanning tunneling spectroscopy," *Phys. Rev. B* **68**, 045422 (2003).
- 28 C. W. Choi and K. P. Ishwar, "Flame stretch effects on partially premixed flames," *Combust. Flame* **123**, 119–139 (2000).
- 29 J. Tersoff and D. R. Hamann, "Theory and application for the scanning tunneling microscope," *Phys. Rev. Lett.* **50**, 1998 (1983).
- 30 Luxel Corporation, Vapor pressure chart, <https://luxel.com/wp-content/uploads/2013/04/Luxel-Vapor-Pressure-Chart.pdf>, 2013.
- 31 P. M. Woodward, A. W. Sleight, and T. Vogt, "Structure refinement of triclinic tungsten trioxide," *J. Phys. Chem. Solids* **56**, 1305–1315 (1995).
- 32 T. Siciliano *et al.*, "WO<sub>3</sub> gas sensors prepared by thermal oxidation of tungsten," *Sens. Actuators, B* **133**, 321–326 (2008).